

Optimal Point Planning for Abundance Estimation of Polymetallic Nodules

Bharath Kalyan, Varadarajan Ganesan, Mandar Chitre and Hari Vishnu
Keppel-NUS Corporate Laboratory and Acoustic Research Laboratory,
National University of Singapore, Singapore 119222
Email: {bharath, mandar, hari}@arl.nus.edu.sg

Abstract—Seabed minerals in form of ferromanganese or polymetallic nodules (PMN) have been reported in the Pacific, Atlantic, and Indian oceans. The distribution of these PMN are influenced by several factors, such as the associated topographic undulations, surface chlorophyll levels, sediment type and thickness, and water depth. Traditionally, determination of the existence and the distribution of PMN involves a series of surveying and sampling operations carried out using geophysical techniques from ships, complemented by sampling devices such as benthic corers and near-bottom photography. However, given the vastness of the region in question, the Clarion Clipperton fracture zone (CCFZ), it is practically infeasible to survey the entire region for PMN distribution. This paper focuses on various strategies to choose optimal points for future exploration studies, so as to build maps that closely represent the spatial distribution of PMN in the region.

I. INTRODUCTION

Polymetallic nodules (PMN) in the deep sea have received increasing attention in the recent years due to presence of several economically valuable elements such as manganese, nickel, copper, cobalt and lead. Factors such as nodule grade, abundance, their accessibility, and the relative geographical proximity to USA have led to a concentration of activity in the northeastern equatorial Pacific region known as the Clarion-Clipperton Fracture Zone (CCFZ) [1]–[3]. The CCFZ is a large region spanning over approximately 9 million square kilometers stretching between Baja California and the Hawaiian Islands from east to west, and the Clarion and Clipperton fracture zones from north to south as shown in Fig. 1. The distribution of PMN within this region is by no means uniform. This is attributed to various environmental factors such as the associated topographic undulations, surface chlorophyll levels, sediment type and thickness, and water depth [2], [4].

Many national institutes and consortia of international companies have explored PMN in CCFZ and data have been collected using various sampling, near-bottom photography and acoustic techniques to estimate nodule abundance [5]–[9]. However, given the vastness of the region it is not practically possible to survey the entire region for PMN distribution. In order to plan exploration and exploitation efficiently in such a large area, we need to build a spatial distribution map of these PMN resources. The International Seabed Authority (ISA) recognizing the importance of spatial distribution maps convened a workshop to establish a geological model of PMN deposits in the CCFZ [10]. Furthermore given a spatial

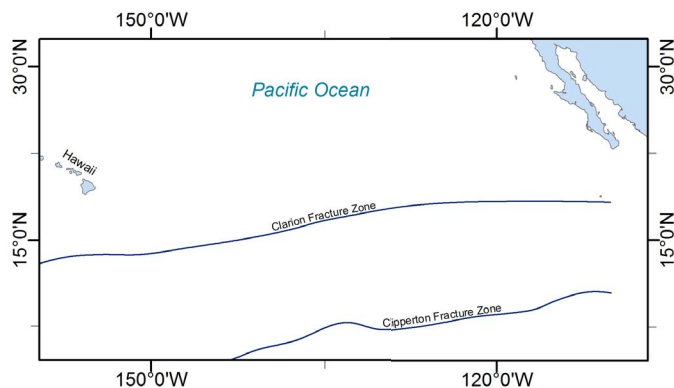


Fig. 1. Region of interest: Clarion Clipperton Fracture Zone

distribution map of the region, we would also need to develop suitable strategies to choose points for future exploration so as to reduce the uncertainty in these maps, which is the problem addressed in this paper.

In this paper, we present various strategies to determine sampling locations for future exploratory studies so as to maximize the amount of information obtained. In other words, we aim to reduce the uncertainty of an existing spatial distribution map, thereby representing spatial distribution of PMN resources closer to the ground truth. Prior to determining future sampling locations, we need to predict the nodule density in regions where no data is available using the data points where nodule density has been obtained using free-fall grab recoveries from past exploratory cruises. Informally speaking, we need to interpolate the ground truth values of nodule density to predict the nodule density in regions where no information is available. The traditional approach adopted in the literature of geostatistics is to estimate the spatial distribution of variables, i.e., nodule density in this case, using kriging techniques and its variants [7], [11], [12]. An advantage of using kriging or its variants is that, they provide an uncertainty value associated with each estimate. It is this uncertainty that we eventually exploit to predict sampling locations. By choosing optimal sampling points, we minimize mission time and at the same time maximize the information gain which helps in building accurate maps. Here, we approach the optimal point planning problem in two different ways:

- 1) Sequential point planning - a strategy where k number

of points are planned in a sequential manner, where each subsequent point for sampling is planned only after the previous point has been sampled.

- 2) Parallel point planning - a strategy where k number of points are planned simultaneously. Furthermore, we formulate a genetic algorithm and a simulated annealing based approach to determine the multiple points simultaneously.

We also discuss the effectiveness of both the methods on being able to build maps with low uncertainty.

The paper is organized as follows. Section II gives a brief description of the PMN resource estimation technique using kriging, while section III, discusses the various point planning strategies. The results from these point planning strategies are presented and the efficacies are compared in section IV to draw conclusions in section V.

II. PMN RESOURCE ESTIMATION

The PMN resource estimation is based on a data gathered from various publicly available databases [13], [14]. The data consists of primarily individual free-fall grab recoveries at various stations across CCFZ gathered over the past 50 years from various cruises. The method used in the resource estimation and the results obtained are presented in the following section.

A. Kriging

Kriging is an interpolation technique that uses a weighted average of known neighbouring samples to estimate the unknown value (PMN density in our case) at a given location [11], [15]. It assumes that the distance or direction between sample points reflects a spatial correlation that can be used to explain variation in the surface. Formally, the kriging estimator can be written as follows:

$$\hat{Z}(u_o) = \hat{Z}_o = \sum_{i=1}^N w_i Z(u_i) = \sum_{i=1}^N w_i Z_i \quad (1)$$

$$= [w_1 \quad \cdots \quad w_n] \begin{bmatrix} z_1 \\ \vdots \\ z_n \end{bmatrix} = \mathbf{w}^T \mathbf{Z} \quad (2)$$

where, $Z(u_i)$ or simply Z_i is the measured PMN density at location u_i , w_i is the unknown weight that needs to be determined, and $\hat{Z}(u_o)$ is the estimated PMN density at location u_o . The main idea behind kriging is to determine the weights \mathbf{w} , that minimizes the prediction variance (kriging variance) of the estimator, i.e.,

$$\begin{aligned} \min : \sigma_\epsilon^2 &= \text{Var}(Z_0 - \hat{Z}_0) = \mathbb{E}[(Z_0 - \hat{Z}_0)^2] \\ \text{s.t.} \quad \mathbb{E}[Z_0 - \hat{Z}_0] &= 0. \end{aligned} \quad (3)$$

Essentially, the error associated with the estimated value of PMN density needs to be minimised. The solution that meets this criterion is given by,

$$\mathbf{w} = \mathbf{C}^{-1} \mathbf{D}, \quad (4)$$

where \mathbf{C} is the matrix of covariances between measured data points, \mathbf{D} is a vector of covariances between measured data points and the estimated point. The elements of the covariance matrix and the vector are functions of distances between the respective points.

$$C_{ij} = f(\|u_i - u_j\|) \quad (5)$$

$$D_i = f(\|u_i - u_o\|) \quad (6)$$

The function f describes the degree of spatial dependence of a random field (PMN density in our case) by calculating the variance of the difference between the random variables at two locations. The spatial variability of the attribute is expressed by a variogram, which is estimated from the measured data using the semi-variance given in (7). The semivariogram is defined as a function of separation distances among measurements, also known as *lag h* [15]. Formally, it is defined as follows:

$$\hat{\gamma}(h) = \frac{1}{2|N(h)|} \sum_{(u_i, u_j) \in N(h)} |Z(u_i) - Z(u_j)|^2 \quad (7)$$

where $N(h)$ is the number of data points that are h units apart from one another. A functional fit is performed on these discrete values of the semivariogram at different lag, h , using a spherical function of the form,

$$\gamma(h) = a + (\sigma^2 - a) \left\{ \frac{3h}{2r} - \frac{h^3}{2r^3} \right\} \quad (8)$$

where a and σ^2 indicate the values of the semivariogram function at zero lag (known as *nugget*) and the maximum possible value (known as *sill*) respectively. r is the upper bound on lag h or alternatively the lag distance at which the semivariogram reaches the sill value, that we specify and believe that the data beyond this lag is not correlated. Thus with the functional form of semivariogram, we determine the kriging weights with (4). Following this, the PMN density is estimated at unknown locations

$$\hat{\mathbf{Z}} = \mathbf{w}^T \mathbf{Z} \quad (9)$$

with an uncertainty associated with the estimated values,

$$\sigma_\epsilon^2 = \sigma^2 - \mathbf{w}^T \mathbf{D}. \quad (10)$$

The kriged estimates of PMN distribution across the entire CCFZ are shown in Fig. 2 (a) using a database that was built, with 645 sampling stations. It is important to note that the kriged estimates of nodule density would not be identical to the map generated by ISA, as more than 8000 sample points (including proprietary databases) were used to generate the ISA kriged map [7]. Based on the PMN density estimates and their associated uncertainties, as illustrated in Fig. 2, optimal point planning strategies are formulated to reduce the error associated with the estimated values.

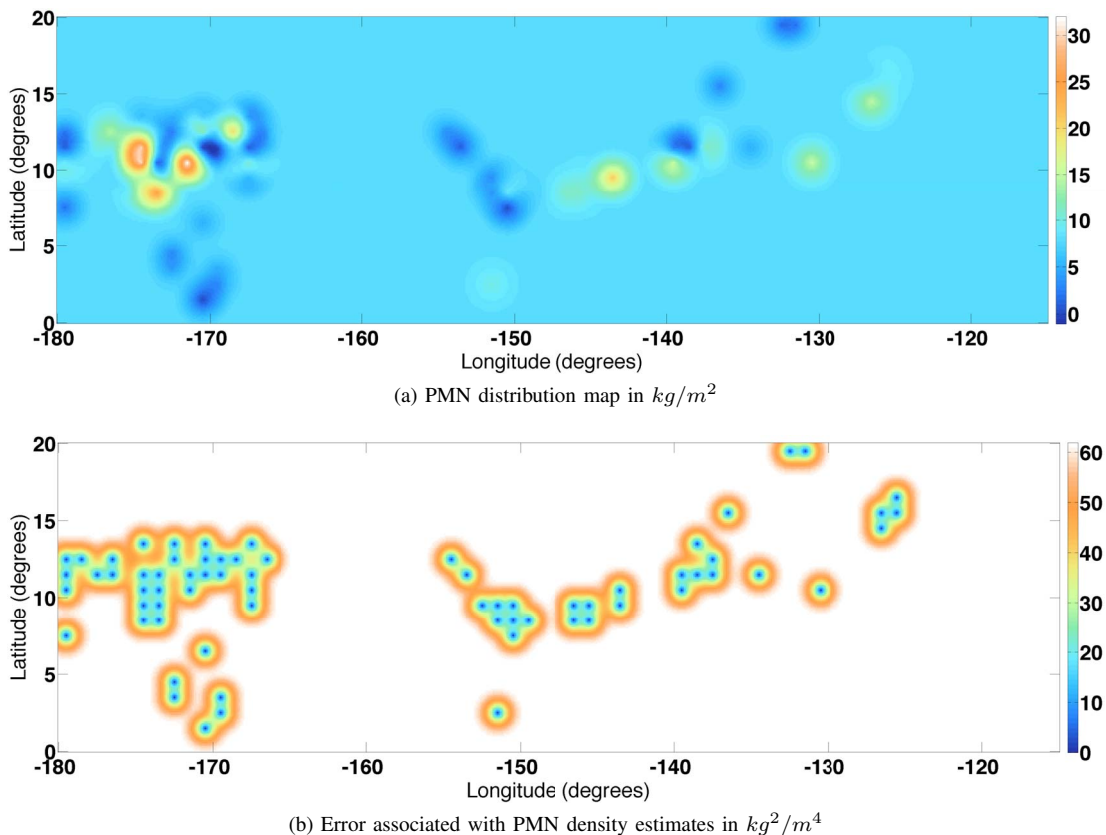


Fig. 2. Krigged output: PMN density estimates along with their associated uncertainties across CCFZ.

III. OPTIMAL POINT PLANNING

The primary focus of this paper is to be able to suggest optimal sampling points for future cruises. The reason for delving into kriging techniques in the earlier section is that they provide the uncertainty associated with their predictions given in (10). We exploit this uncertainty and plan points that try to maximise information gain during future explorations. By doing so, we also minimise the error associated with the estimated values which in turn increases the accuracy of the spatial distribution maps being built. As mentioned earlier, there are two different methods that can be adopted for point planning: a sequential approach and a parallel approach. We describe both the approaches and compare their effectiveness in the following sections.

A. Sequential Point Planning

In the sequential point planning method, as the name suggests, points are planned in a sequential manner. Each point is first visited and sampled for nodule density following which the subsequent point is planned. A more formal procedure is described as follows:

As illustrated in algorithm 1, a brute-force search technique is employed to determine the optimal point by sampling all points in the map and calculating the one that yields the minimum total error across the entire map. We carried out simple kriging and then calculated the subsequent points that need to be sampled based on the strategy suggested above.

Algorithm 1: Sequential point planning

Result: $\min \sum_g \sigma_\epsilon^2$
initialize N : No. of sequential points to be planned;
for ($i = 0$; $i < N$; $i = i + 1$) **do**
 determine $u_i | \min \sum_g \sigma_\epsilon^2$;
 update C matrix & D vector;
 measure nodule density at u_i ;
end

Since we cannot physically measure the nodule density at the planned points, here in our simulations we assume the ground-truth to be equal to the average value of the nodule density in that region. Following this, we calculate the subsequent points. The resulting map of sequential point planning and the optimal points generated are shown in Fig. 3 (a). Sampling in the suggested locations would yield maps with lower total uncertainty than if sampled at other random locations. In other words, if we were to sample in the suggested locations, the maps hence built should be more accurate and closely represent the ground truth spatial distribution of the nodule density.

B. Parallel Point Planning

Most deep sea mineral exploration cruises do not have the flexibility to determine sampling locations in-situ primarily due to economic constraints, which would be the case if we were to adopt a sequential point planning strategy. Hence, all the points need to be planned in advance which makes it imperative for a parallel point planning approach. The parallel point planning approach can be viewed as a multi-dimensional optimisation problem with the aim of minimising the total uncertainty of the map. The dimensions of the problem are the co-ordinates of different sampling points. To this end, we formulate two variants using genetic algorithm and simulated annealing based approach to calculate the sampling points which would result in lowering the total uncertainty of the map.

1) *Genetic Algorithm*: A genetic algorithm (GA) is a method for solving both constrained and unconstrained optimisation problems based on a natural selection process that mimics biological evolution. The algorithm repeatedly modifies a population of individual solutions. At each step, the genetic algorithm randomly selects individuals from the current population and uses them as parents to produce the children for the next generation. Over successive generations, the population “evolves” toward an optimal solution. Details of the working of a genetic algorithm can be found in [16].

The various elements that were used to formulate the genetic algorithm are as follows:

- 1) *Chromosome encoding*: $[(x_1, y_1), (x_2, y_2), \dots, (x_n, y_n)]$ where (x_i, y_i) are co-ordinates of the sampling points, $i \in [1, n]$, and n is the total number of points that have to be sampled for nodule abundance.
- 2) *Fitness function*: $\frac{1}{\sum_g \sigma_\epsilon^2}$; where $\sum_g \sigma_\epsilon^2$ is the total uncertainty if we were to sample at all n points in a given chromosome. Hence, the aim is to maximise the fitness function (by minimising the total uncertainty).
- 3) *Population size*: 20 Chromosomes
- 4) *Parent selection process*: Roulette wheel selection - The fitter chromosomes have higher chance of getting selected.
- 5) *Crossover operator*: The crossover operator is defined as follows:

$$\begin{aligned} & [(x_1, y_1), \dots, (x_n, y_n)] + [(\hat{x}_1, \hat{y}_1), \dots, (\hat{x}_n, \hat{y}_n)] \\ &= [(x_1, y_1), \dots, (x_{\frac{n}{2}}, y_{\frac{n}{2}}), (\hat{x}_{\frac{n}{2}+1}, \hat{y}_{\frac{n}{2}+1}), \dots, (\hat{x}_n, \hat{y}_n)] \\ &+ [(\hat{x}_1, \hat{y}_1), \dots, (\hat{x}_{\frac{n}{2}}, \hat{y}_{\frac{n}{2}}), (x_{\frac{n}{2}+1}, y_{\frac{n}{2}+1}), \dots, (x_n, y_n)] \end{aligned} \quad (11)$$

where the offsprings have half the number of points of either parent. The crossover rate, $P_{cr} = 0.7$.

- 6) *Mutation*: The co-ordinates of the points (x_i, y_i) in a chromosome are altered by a small value $\delta \in [-1, 1]$ with a finite probability P_m . The mutation rate, $P_m = 0.1$.

- 7) *Elitist strategy*: Fittest chromosome (one chromosome in this case) is always retained if it undergoes any change during the evolutionary process.

The population was allowed to evolve over 200 generations (iterations). The fittest chromosome at the end of the evolutionary process is the set of points where the sampling needs to be carried out so as to obtain a PMN density map with the least uncertainty. The points which correspond to the fittest chromosome at the end of evolutionary process are shown in Fig. 3 (b).

2) *Simulated Annealing*: Simulated annealing (SA) is a method for solving unconstrained and bound-constrained optimisation problems. The method models the physical process of heating a material and then slowly lowering the temperature to decrease defects, thus minimising the system energy. At each iteration of the simulated annealing algorithm, a new point is randomly generated. The distance of the new point from the current point, or the extent of the search, is based on a probability distribution with a scale proportional to the temperature. The algorithm accepts all new points that lower the objective function $\left(\sum_g \sigma_\epsilon^2, \text{ the total uncertainty in our case} \right)$,

but also, with a certain probability, points that raise the objective. By accepting points that raise the objective, the algorithm avoids being trapped in local minima, and is able to explore globally for more possible solutions. An annealing schedule is selected to systematically decrease the temperature as the algorithm proceeds. As the temperature decreases, the algorithm reduces the extent of its search to converge to a minimum. The details of the algorithm can be found in [17].

As opposed to the considerable number of hyper parameters that needs to be tuned in a genetic algorithm, there are only a few hyper parameters associated with the SA approach. This makes a SA approach simpler and neater. Similar to GAs, at the end of the annealing process, the system converges to a minima. In other words, we get the points that need to be sampled such that the resulting map of nodule density would have the least uncertainty (high accuracy). Figure 3 (c) shows the optimal sampling locations that have been generated by using SA.

IV. RESULTS & DISCUSSION

The PMN resource estimation is based on a data gathered from various publicly available databases [13], [14]. The data consists of primarily individual free-fall grab recoveries at various stations across CCFZ gathered over the past 50 years from various cruises. Based on this data, a kriged nodule distribution map along with an associated uncertainty map is generated for the entire CCFZ region, as illustrated in Fig. 2. The generated uncertainty map in Fig. 2 (b) forms the basis for our optimal point planners. It can be seen from Fig. 3 that all the points planned from different point planners are in the regions of high uncertainty. It is also intuitive that sampling in regions where no information is available (uncertainty is high) tends to reduce the uncertainty of the resulting map. Also, it

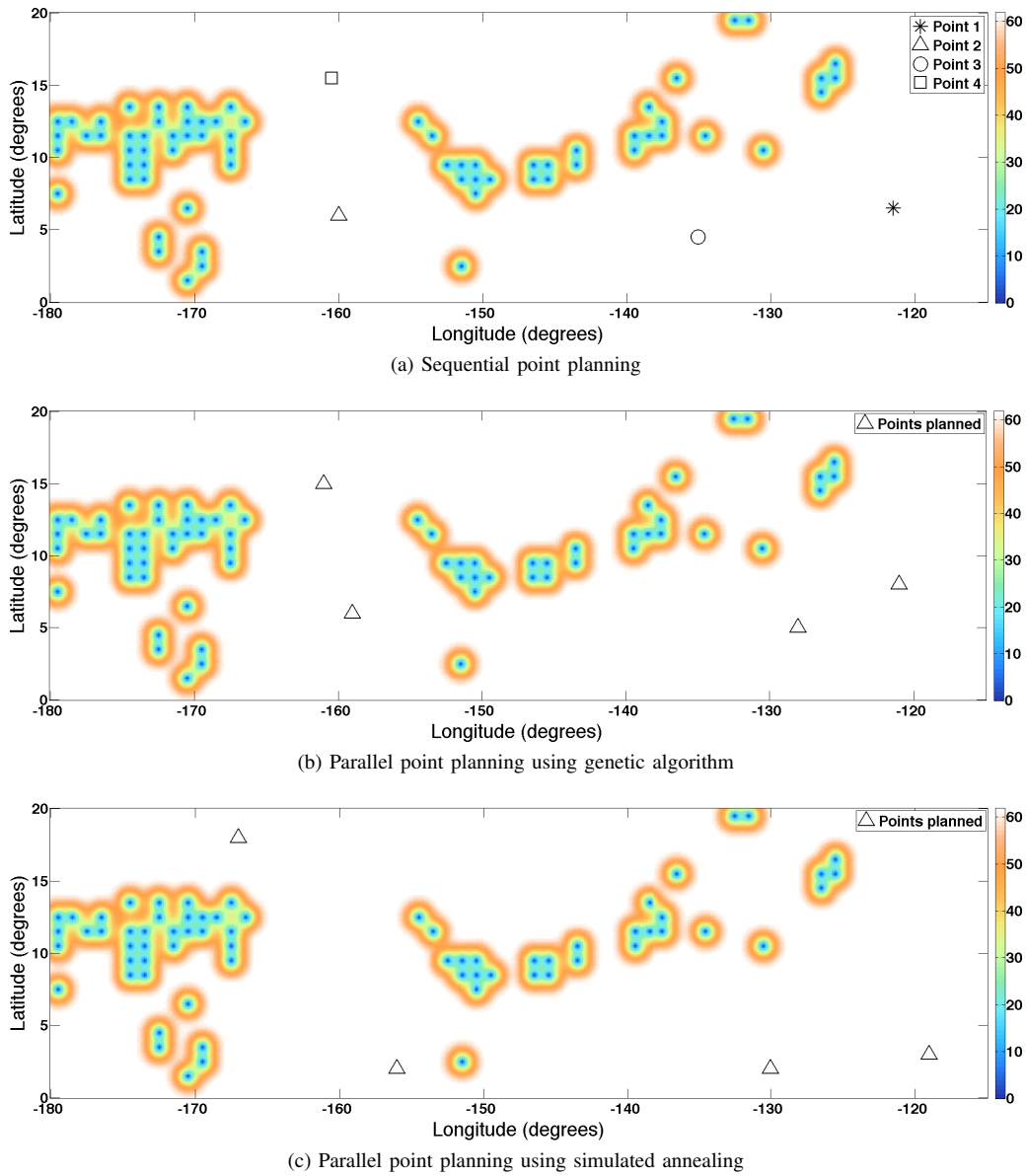


Fig. 3. Output of sequential & parallel optimal point planning algorithms overlaid on the uncertainty map (kg^2/m^4) across the CCFZ.

can be observed from Fig. 3 that the points planned by the different algorithms are different. Hence, there is a need to quantify which method performs better. For this we analyse the total uncertainty of the generated maps, if the locations suggested by the different algorithms were sampled.

Figure 4 shows the boxplot of the total resulting uncertainties, if sequential planning strategy and parallel planning strategy (GA and SA) were adopted for point planning across CCFZ. It needs to be noted that the sequential planning approach yields a constant total uncertainty. However, GAs and SA approaches can yield different values of total uncertainty every time due to converging into different local minima, as it is difficult to converge at the global optimum, especially in higher dimensions (also known as the curse of dimensionality). We view the optimal point planning in the CCZ as a higher

dimensional problem since 4 points (8 dimensions, one for each co-ordinate) were involved. It can be seen from Fig. 4 that the parallel point planning strategies out perform the sequential point planning strategy. And between GA and SA, GA performs better than SA. The difference in performance of GA and SA for different conditions can be attributed to the fact that SA only relies on “mutation” to span the search space and hence it becomes increasingly difficult to find an optimal solution in higher dimensions. On the other hand, GAs can make use of the crossover feature to span the search space more effectively in higher dimensional problems. It has also been noted that for lower dimensional problems, the simplicity of the SA approach allows for convergence at the global optimum as opposed to the number of hyper parameters that need to be tuned in GA.

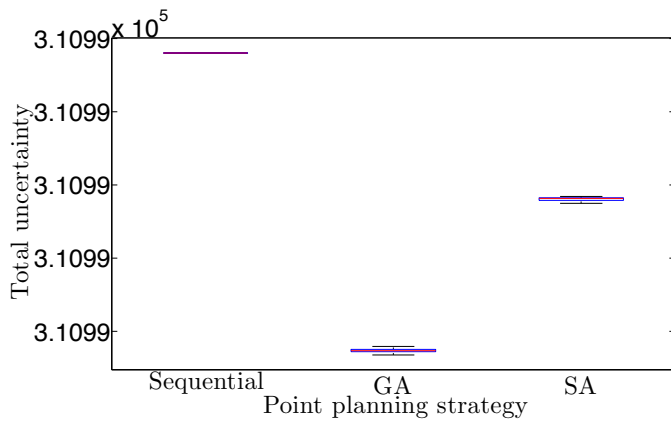


Fig. 4. Box plot of total uncertainty for different point planning strategies in the CCFZ. GA and SA were executed 20 times each.

V. CONCLUSION

With the aim of planning sampling points for exploratory studies, we have delved into different statistical techniques to predict PMN resources across CCFZ using limited data, in form of kriging. Kriging also gives an uncertainty associated with the estimated PMN density values. We exploit these uncertainty values and formulate a strategy to plan points for future exploration so as to build more accurate maps of nodule density. We have also explored different point planning strategies in the form of sequential and parallel point planning and compared the effectiveness of each method. Furthermore in our work on PMN resource exploration, we are also concurrently working on building a geological model of PMN distribution based on our understanding of nodule formation and other available environmental parameters [18]. In future, there are plans to incorporate the output of this geological model into the optimal point planner, instead of simple kriging.

ACKNOWLEDGMENT

The authors thank the National Research Foundation, Keppel Corporation and National University of Singapore for supporting this work done in the Keppel-NUS Corporate Laboratory. The conclusions put forward reflect the views of the authors alone, and not necessarily those of the institutions within the Corporate Laboratory.

REFERENCES

- [1] D. Z. Piper, K. Leong, and W. F. Cannon, "Manganese Nodule and Surface Sediment Compositions: DOMES Sites A, B, And C," in *Marine Geology and Oceanography of the Pacific Manganese Nodule Province*, ser. Marine Science, J. L. Bischoff and D. Z. Piper, Eds. Springer US, 1979, no. 9, pp. 437–473.
- [2] D. S. Cronan, "Deep-sea nodules: distribution and geochemistry," *Marine manganese deposits*, vol. 15, p. 11, 1977.
- [3] T. Marjoram, H. Cameron, G. Ford, A. Garner, and M. Gibbons, "Manganese nodules and marine technology," *Resources Policy*, vol. 7, no. 1, pp. 45–57, Mar. 1981.
- [4] J. Z. Frazer and M. B. Fisk, "Geological factors related to characteristics of sea-floor manganese nodule deposits," *Deep Sea Research Part A. Oceanographic Research Papers*, vol. 28, no. 12, pp. 1533–1551, Dec. 1981.
- [5] J. L. Mero, "Economic aspects of nodule mining," *Marine manganese deposits*, pp. 327–355, 1977, bibtex: mero_economic_1977.
- [6] S. V. Margolis and R. G. Burns, "Pacific Deep-Sea Manganese Nodules: Their Distribution, Composition, and Origin," *Annual Review of Earth and Planetary Sciences*, vol. 4, p. 229, 1976.
- [7] C. L. Morgan, "Resource Estimates of the Clarion-Clipperton Manganese Nodule Deposits," in *Handbook of Marine Mineral Deposits*, D. S. Cronan, Ed. CRC Press, Nov. 1999, pp. 145–170.
- [8] R. Sharma, "Quantitative estimation of seafloor features from photographs and their application to nodule mining," *Marine Georesources & Geotechnology*, vol. 11, no. 4, pp. 311–331, 1993.
- [9] S. H. Lee and K.-H. Kim, "Side-Scan Sonar Characteristics and Manganese Nodule Abundance in the Clarion-Clipperton Fracture Zones, NE Equatorial Pacific," *Marine Georesources & Geotechnology*, vol. 22, no. 1–2, pp. 103–114, 2004.
- [10] "A Geological Model of Polymetallic Nodule Deposits in the Clarion-Clipperton Fracture Zone," ISA Technical Study: No. 6, 2010.
- [11] N. Cressie, "The origins of kriging," *Mathematical geology*, vol. 22, no. 3, pp. 239–252, 1990.
- [12] J. Mucha, M. Wasilewska-Blaszczyk, R. A. Kotlinski, and L. Maciag, "Variability and Accuracy of Polymetallic Nodules Abundance Estimations in the IOM Area - Statistical and Geostatistical Approach." International Society of Offshore and Polar Engineers, Jan. 2013.
- [13] Warnken, Robin R, Virden, William T., and Carla J. Moore, "The NOAA and MMS Marine Minerals Bibliography," 1992. [Online]. Available: <https://data.nodc.noaa.gov/>
- [14] "ISA Central Data Repository." [Online]. Available: <https://www.isa.org/jm/central-data-repository>
- [15] G. Matheron, "Principles of geostatistics," *Economic geology*, vol. 58, no. 8, pp. 1246–1266, 1963.
- [16] M. Mitchell, *An Introduction to Genetic Algorithms*. Cambridge, MA, USA: MIT Press, 1998.
- [17] S. Kirkpatrick, C. D. Gelatt, and M. P. Vecchi, "Optimization by simulated annealing," *Science*, vol. 220, no. 4598, pp. 671–680, 1983.
- [18] H. Vishnu.N, B. Kalyan, and M. Chitre, "Spatial modeling and uncertainty characterization of polymetallic nodules in the Clarion-Clipperton zone," in *Proceedings of OCEANS'17*, Anchorage, USA, 2017.